Eur. Phys. J. Special Topics **160**, 1–10 (2008)

DOI: 10.1140/epjst/e2008-00704-1

THE EUROPEAN PHYSICAL JOURNAL SPECIAL TOPICS

Quantum and classical correlations in tripartite Gaussian states of light

A. Allevi[1,a], M. Bondani[2], M.G.A. Paris[3,4,5], and A. Andreoni[1]

[1] CNR-INFM-CNISM, Dipartimento di Fisica e Matematica, Università degli Studi dell'Insubria, 22100 Como, Italy
[2] National Laboratory for Ultrafast and Ultraintense Optical Science - CNR-INFM, 22100 Como, Italy
[3] Dipartimento di Fisica, Università di Milano, 20133 Milano, Italy
[4] CNISM, U.d.R. Milano Università, 20133 Milano, Italy
[5] Institute for Scientific Interchange Foundation, 10133 Torino, Italy

Abstract. We demonstrate an optical scheme involving two interlinked nonlinear interactions taking place simultaneously in a second-order nonlinear crystal. The three-mode output state is fully inseparable and endowed with perfect photon-number correlations among the generated fields. In order to discriminate between classical and quantum correlations we evaluate the quantum noise reduction, *i.e.* compare the fluctuations of the difference photocurrent between one mode and the sum of the other two with those coming from three uncorrelated coherent states. Preliminary results indicate that our scheme may achieve three-mode sub-shot noise correlations with current technology.

1 Introduction

In the last decade nonlinear interactions involving several modes of radiation have attracted much attention in order to realize all-optical information processing [1] and generate nonclassical states of light [2]. In particular, nonlinear interactions in the quantum regime may be used to generate multimode entangled states. Interest in entanglement has grown recently due to its apparent usefulness as an enabling technology in quantum information and communication protocols such as quantum teleportation [3], dense coding [4,5] and quantum computation [6]. Most of the concepts have been initially developed for discrete quantum variables though, more recently, attention has been also devoted to continuous variable (CV) systems and multiphoton states of light [7,8]. In particular, multipartite CV entanglement has been suggested to realize telecloning [9–11], to enhance communication networks [12] and to improve the discrimination of quantum operations [13].

Several experimental schemes to generate multimode entangled states have been suggested and demonstrated. The first example is provided by the original teleportation experiments in Ref. [14], where one mode of a twin beam was mixed with a coherent state, although no specific analysis was made on the entanglement properties (besides the verification of teleportation). A similar scheme, where one mode of a twin beam is mixed with the vacuum, has been demonstrated and applied to controlled dense coding [15]. Moreover, a fully inseparable three-mode entangled state has been generated and verified by mixing three independent squeezed vacuum states in a network of beam splitters [16]. Recently we suggested and demonstrated a compact scheme to realize three-mode entanglement by means of two interlinked $\chi^{(2)}$ interactions occurring in a single nonlinear crystal in a type-I non-collinear phase-matching geometry [17].

[a] e-mail: alessia.allevi@uninsubria.it

Other schemes involving cascaded interactions have been also analyzed theoretically either in periodically poled crystals [18] or in second-order nonlinear ones [19,20]. Notice, however, that the use of a single nonlinear medium makes the system more compact and robust compared to other schemes suggested and demonstrated so far, in which additional parametric sources and linear devices, such as beam splitters, introduce unavoidable losses.

In this paper we review the generation scheme and address the characterization of the three-mode state at the output. We will not deal with characterization of entanglement. Rather we focus on correlations in the photon number and analyze in some details the possibility of revealing sub-shot-noise correlations among the three modes. As we will see theoretically, and on the basis of preliminary experimental results, our scheme is suitable to detect nonclassical correlations with current technology.

The paper is structured as follows. In section 2 we report the theoretical description of our scheme, together with the evaluation of intensity correlations. In section 3 we describe the experimental setup and report the experimental results. Section 4 closes the paper with some concluding remarks.

2 Theory

In our scheme two interlinked interactions, namely a spontaneous parametric downconversion (SPDC) process and a sum-frequency generation, are taking place simultaneously in a single nonlinear crystal. Five fields a_j are involved in the interactions, two of which, say a_4 and a_5, are considered as non-evolving pumps and thus are treated within the parametric approximation and included in the coupling coefficients. The effective Hamiltonian that describes our interaction scheme is given by

$$H_{\rm int} = \gamma_1 a_1^\dagger a_3^\dagger + \gamma_2 a_2^\dagger a_3 + h.c., \tag{1}$$

where γ_1 and γ_2 are coupling coefficients. The earliest studies on the dynamics and quantum properties of the states realized via this Hamiltonian can be traced back to the works in Refs. [21]. The relevance in studying the dynamics generated by the above Hamiltonian in details lies in the fact that it can be realized in a variety of different contexts, from quantum optics [11,18,20,22] to condensate physics [23]. Studies have been also performed in which the coupling between two optical modes and a vibrational mode of a macroscopic object, such as a mirror, has been considered [24]. Recently, also ions trapped in a cavity have been demonstrated to realize the Hamiltonian in Eq. (1) for a suitable configuration [25].

The Hamiltonian admits the following conservation law of photon numbers $N_{1,2,3}$

$$\Delta(t) \equiv N_1(t) - N_2(t) - N_3(t) \equiv \Delta(0). \tag{2}$$

If we take the vacuum $|\mathbf{0}\rangle \equiv |0\rangle_1 \otimes |0\rangle_2 \otimes |0\rangle_3$ as the initial state, we have

$$N_1(t) = N_2(t) + N_3(t) \tag{3}$$

$\forall t$, being $N_{\rm j}(t) = \langle a_{\rm j}^\dagger(t) a_{\rm j}(t)\rangle$ the mean number of photons in the j-th mode. Under these hypotheses the evolved state at any time t can be written as

$$|\mathbf{T}_0\rangle = U_t|\mathbf{0}\rangle = \frac{1}{\sqrt{1+N_1}} \sum_{mr} \left(\frac{N_2}{1+N_1}\right)^{m/2} \left(\frac{N_3}{1+N_1}\right)^{r/2} \sqrt{\frac{(m+r)!}{m!r!}}\, |m+r, m, r\rangle\,. \tag{4}$$

It can be demonstrated that the state in Eq. (4) is a fully inseparable three-mode Gaussian state [26], i.e. a state that is inseparable with respect to any grouping of the modes, thus permitting realizations of truly tripartite quantum protocols such as conditional twin-beam generation and telecloning [11]. The mean numbers of photons N_j that appear in Eq. (4) can

be obtained by the Heisenberg evolution of the field operators. In particular, by introducing $\Omega = \sqrt{|\gamma_2|^2 - |\gamma_1|^2}$ we have $N_1 = N_2 + N_3$ and

$$N_2 = \frac{|\gamma_1|^2|\gamma_2|^2}{\Omega^4}\left[\cos\Omega t - 1\right]^2 \qquad N_3 = \frac{|\gamma_1|^2}{\Omega^2}\sin^2(\Omega t)\ . \tag{5}$$

We see that when $|\gamma_2|^2 > |\gamma_1|^2$ the dynamics is oscillatory; viceversa, when $|\gamma_1|^2 > |\gamma_2|^2$ we find an exponential behavior.

The state in Eq. (4) is endowed with perfect correlations in the number of photons. The three-mode photon distribution is given by

$$P_T(n,m,r) = \delta_{n,m+r}\frac{1}{1+N_1}\left(\frac{N_2}{1+N_1}\right)^m\left(\frac{N_3}{1+N_1}\right)^r\frac{(m+r)!}{m!r!}, \tag{6}$$

from which we can derive the photon-number correlation coefficients between the components of the entangled state. In particular, due to the conservation law in Eq. (3), we expect the existence of strong intensity correlations among the number of photon n_1 and the sum of the other two, say n_2+n_3. Actually, by exploiting Eq. (6), the corresponding correlation coefficient reads as follows

$$\epsilon_{(1,2+3)} = \frac{\langle n_1(n_2+n_3)\rangle - \langle n_1\rangle\langle n_2+n_3\rangle}{\sqrt{(\langle {n_1}^2\rangle - \langle n_1\rangle^2)\left[\langle (n_2+n_3)^2\rangle - \langle n_2+n_3\rangle^2\right]}} = \frac{N_1(1+N_1)}{N_1(1+N_1)} \equiv 1. \tag{7}$$

Eq. (7) shows that $\epsilon_{1,2+3}$ is identically equal to 1 and thus it does not depend on the number of photons generated by the interlinked interactions. Moreover, if we calculate the partial photon-number correlations, namely between n_1 and n_2 or n_1 and n_3 or again n_2 and n_3, we obtain expressions similar to that reported in Eq. (7), but, in general, they do depend on the mean number of photons involved:

$$\begin{aligned}
\epsilon_{(1,2)} &= \frac{\langle n_1n_2\rangle - \langle n_1\rangle\langle n_2\rangle}{\sqrt{(\langle {n_1}^2\rangle - \langle n_1\rangle^2)\left[\langle {n_2}^2\rangle - \langle n_2\rangle^2\right]}} = \frac{N_2(1+N_1)}{\sqrt{N_1(1+N_1)N_2(1+N_2)}} \overset{N_1\gg 1}{\longrightarrow} \sqrt{\frac{N_2}{1+N_2}} \overset{N_2\gg 1}{\longrightarrow} 1 \\
\epsilon_{(1,3)} &= \frac{\langle n_1n_3\rangle - \langle n_1\rangle\langle n_3\rangle}{\sqrt{(\langle {n_1}^2\rangle - \langle n_1\rangle^2)\left[\langle {n_3}^2\rangle - \langle n_3\rangle^2\right]}} = \frac{N_3(1+N_1)}{\sqrt{N_1(1+N_1)N_3(1+N_3)}} \overset{N_1\gg 1}{\longrightarrow} \sqrt{\frac{N_3}{1+N_3}} \overset{N_3\gg 1}{\longrightarrow} 1 \\
\epsilon_{(2,3)} &= \frac{\langle n_2n_3\rangle - \langle n_2\rangle\langle n_3\rangle}{\sqrt{(\langle {n_2}^2\rangle - \langle n_2\rangle^2)\left[\langle {n_3}^2\rangle - \langle n_3\rangle^2\right]}} = \frac{N_2N_3}{\sqrt{N_2(1+N_2)N_3(1+N_3)}} \overset{N_3\gg 1}{\longrightarrow} \sqrt{\frac{N_2}{1+N_2}} \overset{N_2\gg 1}{\longrightarrow} 1.
\end{aligned} \tag{8}$$

As the detectors we used to perform the correlation measurements are not ideal, we would rewrite the expressions in Eqs. (7) and (8) by taking into account the non-unitary quantum efficiency of the detection apparatus. In particular, let us assume that the photodetection on the three arms is performed with the same quantum efficiency η and without dark counts. The probability operator-valued measure (POVM) of each detector, describing the statistics of detected photons, is thus given by a Bernoullian convolution of the ideal number operator spectral measure

$$\hat{\Pi}_{m_j} = {\eta_j}^{m_j}\sum_{n_j=m_j}^{\infty}(1-\eta_j)^{n_j-m_j}\binom{n_j}{m_j}\,|n_j\rangle\langle n_j| \tag{9}$$

with $j = 1, 2, 3$. As it was extensively derived in Ref. [27], Eq. (9) can be exploited to calculate the expressions of the number of detected photons m_j and of its variance $\sigma^2(m_j)$ in terms of the number of photons n_j and its variance $\sigma^2(n_j)$

$$\hat{m}_j = \eta_j\hat{n}_j, \qquad \sigma^2(m_j) = \eta_j^2\sigma^2(n_j) + \eta_j(1-\eta_j)\langle\hat{n}_j\rangle. \tag{10}$$

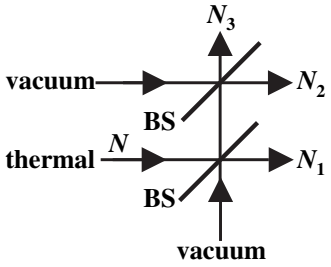

Fig. 1. Generation of a separable three-mode classical state obtained by sending a thermal state $|\nu\rangle$ on two subsequent beam-splitters (BS) whose second port is left unexcited $|0\rangle$.

We notice that, in general, the statistical distribution of the number of detected photons is different from that of the number of photons. Nevertheless, the correlation coefficients calculated for the detected photons can also assume high values; in particular, the correlation coefficient calculated between m_1 and the sum $m_2 + m_3$ reads as follows

$$\epsilon^{m}_{1,2+3} = \frac{\eta^2(1+N_1)N_1}{\sqrt{\eta^2 N_1^2(1+\eta N_1)^2}} = \frac{\eta(1+N_1)}{(1+\eta N_1)} \stackrel{N_1\to\infty}{\longrightarrow} 1 \tag{11}$$

where we have supposed that the detectors have the same quantum efficiency η.

As it has been already noticed for the bipartite case [27], however a high value of the correlation index is not sufficient to discriminate between quantum and classical correlations. As for example, the state generated by sending a thermal state on two subsequent beam-splitters (see Fig. 1), whose second port is left unexcited, is classical but it shows large correlations. In fact, in the ideal case in which the quantum efficiency is equal to 1 and the transmittance of the beam-splitters is $\tau_1 = \tau_2 = 1/2$, it can be demonstrated that the correlation coefficient calculated between the photons exiting the first beam-splitter and the sum of those exiting the second one can be expressed as follows

$$\epsilon_{\mathrm{BS},1,2+3} = \frac{N}{2+N} = \frac{N_1}{1+N_1} \stackrel{N_1\to\infty}{=\!\!=\!\!\longrightarrow} 1 \tag{12}$$

where N represents the mean number of photons of the input thermal state and N_1 is the output at the first beam-splitter. Analogously, by supposing that the detectors placed at each output port of the beam-splitters are characterized by the same quantum efficiency η, Eq. (12) can be rewritten as

$$\epsilon^{m}_{\mathrm{BS},1,2+3} = \frac{\eta N}{2+\eta N} = \frac{\eta N_1}{1+\eta N_1} \stackrel{N_1\to\infty}{=\!\!=\!\!\longrightarrow} 1 \tag{13}$$

for the detected photons.

A good marker of non-classicality can be obtained by considering the difference photocurrent $\hat{D} = \hat{m}_i - \hat{m}_j$, being $m_j = \eta_j n_j$ the number of detected photons on field a_j [28]. In particular, to prove the quantum nature of our tripartite state, we have to study the difference d between the photocurrent relative to field a_1 and the photocurrents relative to the sum of fields a_2 and a_3. In an experiment in which $\eta_1 = \eta_2 = \eta_3$, if the variance of the difference photocurrent $\sigma^2(d = m_1 - (m_2 + m_3))$ is smaller than the sum of the photons detected in the three fields, namely

$$\sigma^2(m_1 - (m_2 + m_3)) < \langle m_1 + (m_2 + m_3)\rangle, \tag{14}$$

the generated state is endowed with non-classical properties. Note that, in general, this demonstration of the quantum nature of a state does not, in general, imply entanglement. In fact, to prove entanglement it would be necessary to reconstruct the entire statistics [29] of the state by means of quantum tomography or to realize a true tripartite quantum protocol [12]. Nevertheless, for states generated by the Hamiltonian in Eq. (1), the existence of sub-shot noise (nonclassical) photon-number correlations is a sufficient condition for entanglement,

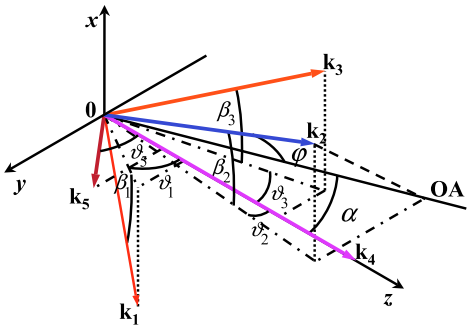

Fig. 2. Scheme of the phase-matched interlinked interactions: (x, y)-plane coincides with the crystal entrance face; α, tuning angle; $\beta_{\rm j}$'s, angles to (y, z)-plane; $\vartheta_{\rm j}$'s, angles on the (y, z)-plane; φ, angle to the optical axis (OA).

i.e. the condition of negative partial transpose is subsumed by the condition of sub-shot noise correlations [11]. We define, as the noise reduction R, the ratio of the left- to right-members of the inequality in Eq. (14). Notice that we must not expect the same behavior for the difference photocurrents between only two of the three fields: in particular, it is possible to demonstrate that we never have a value of $R < 1$ for the pair of fields 2 and 3, while in the other two cases there are strong conditions to be satisfied [30]. Namely, for the pair 1 and 2, we have $R < 1$ if and only if $N_3 < \sqrt{2N_2}$ and, for the pair 1 and 3, if and only if $N_2 < \sqrt{2N_3}$. It is interesting to point out that these two conditions are simultaneously satisfied for very small values of the mean photon numbers, that is for both N_2 and N_3 definitely smaller than 2.

3 Experiments

3.1 Experimental setup

To generate the three-mode entangled state in Eq. (4), we realized the two interlinked interactions in a negative uniaxial crystal in a type-I non-collinear phase-matching geometry. The two processes must simultaneously satisfy energy-matching ($\omega_4 = \omega_1 + \omega_3$, $\omega_2 = \omega_3 + \omega_5$) and phase-matching conditions ($\mathbf{k}_4^e = \mathbf{k}_1^o + \mathbf{k}_3^o$, $\mathbf{k}_2^e = \mathbf{k}_3^o + \mathbf{k}_5^o$), where $\omega_{\rm j}$ are the angular frequencies, $\mathbf{k}_{\rm j}$ are the wavevectors and suffixes o, e indicate ordinary and extraordinary field polarizations. We note that it is possible to satisfy these conditions with a number of different sets of frequencies and interaction angles depending on the choice of the nonlinear medium. To simplify calculations, it is convenient to assume that the wavevector $\mathbf{k_4}$ of the pump field a_4 is normal to the crystal entrance face and propagate along the z axis of the medium. With reference to Fig. 2, we assume that the wavevector $\mathbf{k_5}$ of the other pump field a_5 lies in the plane (y, z) formed by the optical axis (OA) of the crystal and the wavevector $\mathbf{k_4}$. We indicate as ϑ_j the angles in the plane (y, z) formed by each wavevector with $\mathbf{k_4}$ and as β_j the angles of each wavevector with respect to this plane. Under these hypotheses, we have $\beta_4 = \vartheta_4 = 0$ and $\beta_5 = 0$. In order to calculate a set of angles suitable for the realization of the process, it is convenient to write the projection of the phase-matching conditions along the three cartesian axes (x, y, z). We thus obtain two systems, each formed by three equations, *i.e.*

$$\begin{aligned} &k_1 \sin\beta_1 + k_3 \sin\beta_3 = 0, \qquad k_1 \cos\beta_1 \sin\vartheta_1 + k_3 \cos\beta_3 \sin\vartheta_3 = 0, \\ &k_1 \cos\beta_1 \cos\vartheta_1 + k_3 \cos\beta_3 \cos\vartheta_3 = k_4 \end{aligned} \tag{15}$$

for the SPDC, and

$$\begin{aligned} &k_2 \sin\beta_2 = k_3 \sin\beta_3, \qquad k_2 \cos\beta_2 \sin\vartheta_2 = k_3 \cos\beta_3 \sin\vartheta_3 + k_5 \sin\vartheta_5, \\ &k_2 \cos\beta_2 \cos\vartheta_2 = k_3 \cos\beta_3 \cos\vartheta_3 + k_5 \cos\vartheta_5 \end{aligned} \tag{16}$$

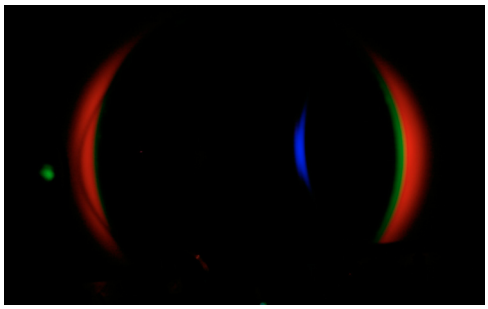

Fig. 3. Colour picture, on a white screen located beyond the nonlinear crystal, of the fields generated by the interlinked interactions taken with a digital camera.

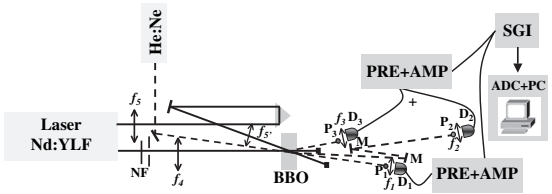

Fig. 4. Scheme of the experimental setup: BBO, nonlinear crystal; NF, variable neutral-density filter; P_{1-3}, pin-holes; $f_{1-5,5'}$, lenses; D_{1-3}, p-i-n photodiodes; M, Aluminum mirrors; PRE+AMPL, low-noise charge-sensitive pre-amplifiers followed by amplifiers; SGI, synchronous gated-integrator; ADC+PC, computer integrated digitizer.

for the other interaction, to which we have to add the following definitions

$$k_2(\alpha,\vartheta_2,\beta_2)=\frac{\omega_2}{c}n_2(\alpha,\vartheta_2,\beta_2)=\frac{\omega_2}{c}\left(\frac{\cos^2(\alpha-\vartheta_2)\cos^2(\beta_2)}{n_o^2(\omega_2)}+\frac{1-\cos^2(\alpha-\vartheta_2)\cos^2(\beta_2)}{n_e^2(\omega_2)}\right)^{-1/2}$$

$$k_4(\alpha)=\frac{\omega_4}{c}n_4(\alpha)=\frac{\omega_4}{c}\left(\frac{\cos^2\alpha}{n_o^2(\omega_4)}+\frac{\sin^2\alpha}{n_e^2(\omega_4)}\right)^{-1/2}. \tag{17}$$

As we have 8 variables and only 6 equations, we can solve the two systems for example by fixing ϑ_5 and α [31]. To experimentally realize the two interactions, we adopted a tuning angle $\alpha = 38.4$ deg and we chose to send the pump field a_5 at an external angle $\vartheta_{5,ext} = -24.47$ deg with respect to the other pump field. For the sake of clarity, in Fig. 3 we show a colour picture of the outputs of the crystal taken with a non-professional digital camera for $\lambda_4 = 349$ nm and $\lambda_5 = 1047$ nm. In particular, it is possible to see both the tunable brilliant downconversion cones and the two polychromatic half-moon-shaped states generated by the upconversion process [31]. To perform our measurements we decided to consider the solutions of Eq. (15) and (16) in the plane (y, z), horizontal in the experiment, for $\lambda_1 = 632.8$ nm, $\lambda_2 = 446.4$ nm and $\lambda_3 = 778.2$ nm, thus obtaining the following external interaction angles with respect to the pump field a_4: $\vartheta_{1,ext} = -9.78$ deg, $\vartheta_{2,ext} = -3.25$ deg and $\vartheta_{3,ext} = +12.06$ deg.

The pump fields were provided by the outputs of a continuous-wave mode-locked Nd:YLF laser regeneratively amplified at the repetition rate of 500 Hz (High Q Laser Production, Austria): in particular, the third-harmonic pulse (∼4.45 ps pulse-duration) was used as field a_4 in order to generate the downconversion process, whereas the fundamental pulse (∼7.7 ps pulse-duration) as field a_5 in order to generate the upconversion process. As depicted in Fig. 4, both pumps were strongly focused (typical intensity values were ∼5GW/cm^2 for field a_4 and ∼2 GW/cm^2 for field a_5) into a β-BaB_2O_4 crystal (BBO, Fujian Castech Crystals, China, 10 mm × 10 mm cross section, 4 mm thickness) cut for type-I interaction ($\vartheta_{\rm cut} = 38.4$ deg). The required superposition of the two pumps in time was obtained with a variable delay line. Moreover, for alignment purposes, we also exploited the light of a cw He:Ne laser (Melles-Griot,

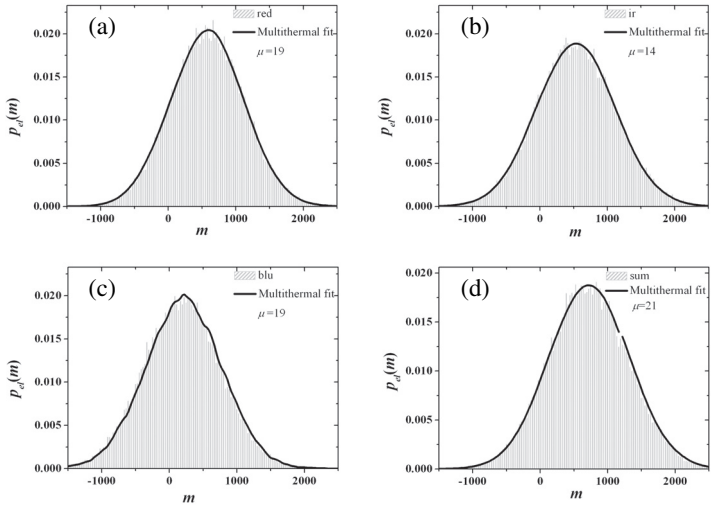

Fig. 5. (a) Histogram of the intensity distribution of the beam at $\lambda_1 = 632.8\,\mathrm{nm}$ together with the multithermal fit. (b) Histogram of the intensity distribution of the beam at $\lambda_3 = 778.2\,\mathrm{nm}$ together with the multithermal fit. (c) Histogram of the intensity distribution of the beam at $\lambda_2 = 446.4\,\mathrm{nm}$ together with the multithermal fit. (d) Histogram of the intensity distribution of the sum $a_2 + a_3$ together with the multithermal fit.

5 mW max output power) to seed the process at the wavelength $\lambda_1 = 632.8\,\mathrm{nm}$. The beam was collimated and sent to the BBO in the plane containing the pumps at the external angle $\vartheta_{1,ext} = -9.78$ deg with respect to a_4. The seeded interactions produced two new fields: a_3 ($\lambda_3 = 778.2\,\mathrm{nm}$, $\vartheta_{3,ext} = 12.06$ deg) generated as the difference-frequency of a_4 and a_1, and a_2 ($\lambda_2 = 446.4\,\mathrm{nm}$, $\vartheta_{2,ext} = -3.25$ deg) generated as the sum-frequency of a_3 and a_5. On the path of the three fields generated by the seeded interactions, we positioned three pin-holes having suitable sizes in order to collect an entangled triplet of single coherence areas produced by operating the system from vacuum (*i.e.* in the absence of any seed fields). In particular, as the size of the coherence areas depends on the pump intensity [26], we optimized the collection of the light by fixing distances and sizes of the pin-holes and by varying the intensity of pump field a_4. In particular, at distances $\mathrm{d}_1 = 60\,\mathrm{cm}$ and $\mathrm{d}_3 = 49\,\mathrm{cm}$ from the BBO two pin-holes of $30\,\mu\mathrm{m}$ diameter were placed so as to be centered with the amplified signal beam at 632.8 nm and with the idler beam at 778.2 nm, respectively. The difference in the value of the distances compensates the different divergence of the two fields due to their different wavelengths. Moreover, as the beam at 446.4 nm has a divergence smaller than those of the other two fields, we selected it by means of a $50\,\mu\mathrm{m}$ diameter pin-hole placed at a longer distance from the crystal, that is $\mathrm{d}_2 = 141.5\,\mathrm{cm}$. The light, suitably filtered by means of bandpass filters located in front of each pin-hole, was focused on each detector by a lens ($f_1 = f_3 = 25\,\mathrm{mm}$, $f_2 = 10\,\mathrm{mm}$). Since we decided to perform our measurements in the macroscopic regime (more than 1000 photons per mode), we used three p-i-n photodiodes (two, $\mathrm{D}_{1,2}$ in Fig. 4, S5973-02 and one, D_3, S3883, Hamamatsu, Japan) as the detectors. In order to obtain the same overall detection efficiency (bandpass filter + detector) on the three arms, we added two adjustable neutral-density filters in the directions of a_2 and a_3, thus obtaining the same value $\eta = 0.45$ on the three arms. The current output of the detectors was amplified by means of low-noise charge-sensitive pre-amplifiers (CR-110, Cremat, Watertown, MA) followed by amplifiers (CR-200-4 μs, Cremat). Being mainly interested in the evaluation of the photon-number correlation between n_1 and the sum $n_2 + n_3$, we connected the detectors D_2 and D_3 to the same amplifier device by means of a BNC T Adapter. The two amplified outputs were integrated by synchronous gated-integrators (SGI in Fig. 4) operating in external trigger modality (SR250, Stanford Research Systems, Palo Alto, CA). The voltage outputs were then sampled, digitized by a 12-bit converter (AT-MIO-16E-1, DAQ National Instruments) and recorded by a computer.

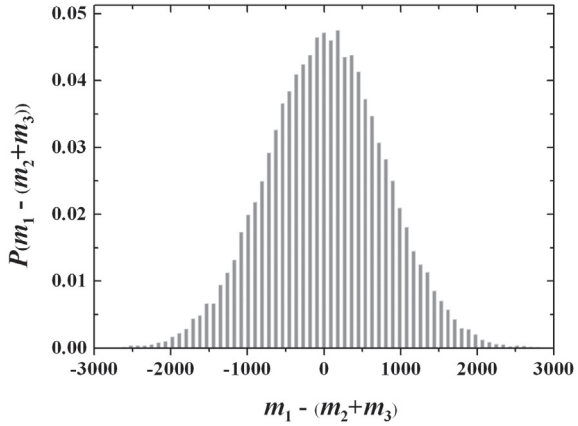

Fig. 6. Distribution of the difference photocurrent, measured over 50000 subsequent laser shots. Note that the distribution was obtained by suitably binning the data in such a way that a single column represents three adjacent channels in the ADC device.

3.2 Experimental results

The distributions of the detected photons collected by the pin-holes are temporally multimode [32]. In fact, the normalized probability distributions reported in Figs. 5(a)–(c) for the three generated fields are well fitted by multithermal distributions obtained by the convolution of μ equally populated thermal modes. These distributions should be characterized by the same number of modes. Actually, we found 19 temporal modes in the coherence area of fields a_1 and a_2 and 14 temporal modes in the coherence area of field a_3. For the distribution of the sum a_2 and a_3, which is reported in Fig. 5(d), we found 21 temporal modes. Note that in order to reconstruct the statistics of a_2 of panel (c) and a_3 of panel (b) separately, we alternatively blocked the light impinging on detectors D_3 and D_2, respectively.

At the pump intensity used in the measurements, the average number of detected photons were: $\langle m_1 \rangle = 605$, $\langle m_2 + m_3 \rangle = 702$, $\langle m_2 \rangle = 170$, and $\langle m_3 \rangle = 520$. The slight disagreement between m_1 and the sum $m_2 + m_3$ (see Eq. (3)) is probably due to the non perfect adjustment of the neutral density filters on the arms of fields a_2 and a_3. Moreover, as the sum of the partial numbers of detected photons m_2 and m_3 is very similar to $m_2 + m_3$, we are quite sure that we realized the same overall quantum efficiency in these two arms.

A preliminary criterion to identify the three modes of the triplet is given by the calculus of the correlation function, even if, as it was remarked in section 2, it represents a necessary but not sufficient condition to establish the entangled nature of the three modes.

The function, written in terms of the detected photons and calculated for $K = 50000$ subsequent laser shots, reads as follows

$$\Gamma(j) = \frac{\sum_{k=1}^{K} \left[(m_1(k) - \langle m_1 \rangle) \left(m_{2+3}(k+j) - \langle m_{2+3} \rangle \right) \right] / K}{\sqrt{\sigma^2(m_1)\sigma^2(m_{2+3})}}, \tag{18}$$

where j and k index the shots, and $\sigma^2(m) = \langle m^2 \rangle - \langle m \rangle^2$ is the variance. Note that, in the regime we used to perform our measurements, Eq. (18) must be corrected by taking into account the presence of noise, both in terms of possible correlation and in terms of increased variance. In details, we calculated the correlation coefficient between m_1 and $m_2 + m_3$, thus obtaining $\epsilon_{1,2+3} = 0.958$. By alternatively blocking the light impinging on detectors D_2 and D_3, we also calculated the partial correlation coefficients between the photons revealed by one of these two detectors and those revealed by D_1. However, in these cases we did not obtain values as high as $\epsilon_{1,2+3}$, namely $\epsilon_{1,2} = 0.714$ and $\epsilon_{1,3} = 0.772$.

The non-classicality of the state generated by the two interlinked interactions can be tested by reconstructing the distribution of the difference photocurrent $d = m_1 - (m_2 + m_3)$, which is

shown in Fig. 6 for our set of data. In particular, we calculate its variance $\sigma^2(d)$ to express the noise reduction

$$R = \frac{{\sigma_d}^2}{\langle m_1 + m_2 + m_3 \rangle}, \tag{19}$$

where, as in the case of the correlation function, the variance of the difference photocurrent must be corrected for the electronic noise in the absence of light. As we remarked in Ref. [28], if $(1-\eta) < R < 1$, the state displays nonclassical correlations. In our case, we obtained $R = 1.81$, a value not too larger than 1, which marks the boundary between classical and non-classical behaviors. This result can be improved not only by optimizing the collection of the coherence areas, but also by adjusting the quantum efficiencies on the arms of a_2 and a_3 through the optimization of the neutral density filters.

4 Conclusions

We have analyzed an optical scheme involving two interlinked nonlinear interactions taking place simultaneously in a $\chi^{(2)}$ nonlinear crystal. The three-mode output state is fully inseparable and endowed with perfect photon-number correlations among the generated fields. We realized the experimental scheme in the macroscopic regime (more than 1000 photons per mode) obtaining some preliminary experimental results. The results could be undoubtedly improved by slightly adjusting some parameters, such as the collection of the single coherence areas on the three modes and the balance of the quantum efficiency in the arms of fields a_2 and a_3. The optimization of these elements would be useful for increasing the photon-number correlations on one hand and for lowering the noise reduction on the other one. The regime of continuous variables in which we operate makes our system particularly promising for several applications: as an example, it can be used for the production of conditional twin-beam states and also for the generation of quasi-Fock states with a number of photons greater than 1. In addition, the scheme is suitable for the realization of imaging protocols, such as image transfer and ghost-imaging.

This work has been supported by MIUR projects FIRB-RBAU014CLC-002 and PRIN-2005024254-002.

References

1. T. Kartaloglu, Z.G. Figen, O. Aytür, J. Opt. Soc. Am. B **20**, 343 (2003) and references therein
2. J. Zhang, C. Xie, K. Peng, Phys. Rev. A **66**, 032318 (2002)
3. C.H. Bennett, G. Brassard, C. Crepeau, R. Jozsa, A. Peres, W.K. Wootters, Phys. Rev. Lett. **70**, 1895 (1993)
4. C.H. Bennett, S.J. Wiesner, Phys. Rev. Lett. **69**, 2881 (1992)
5. T.C. Ralph, E.H. Huntington, Phys. Rev. A **66**, 042321 (2002)
6. D.P. DiVincenzo, Science **270**, 255 (1995)
7. S.L. Braunstein, A.K. Pati, *Quantum Information Theory with Continuous Variables* (Kluwer Academic Publishers, Dordrecht, 2002)
8. A. Ferraro, S. Olivares, M.G.A. Paris, *Gaussian States in Quantum Information*, Napoli Series on Physics and Astrophysics (Bibliopolis, Napoli, 2005) and e-print [`quant-ph/0503237`]
9. M. Murao, D. Jonathan, M.B. Plenio, V. Vedral, Phys. Rev. A **59**, 156 (1999)
10. P. van Loock, S. Braunstein, Phys. Rev. Lett. **87**, 247901 (2001)
11. A. Ferraro, M.G.A. Paris, M. Bondani, A. Allevi, E. Puddu, A. Andreoni, J. Opt. Soc. Am. B **21**, 1241 (2004); A. Ferraro, M.G.A. Paris, Phys. Rev. A **72**, 032312 (2005)
12. P. van Loock, S. Braunstein, Phys. Rev. Lett. **84**, 3482 (2000)
13. G.M. D'Ariano, P. Lo Presti, M.G.A. Paris, J. Opt. B **4**, S273 (2002)
14. A. Furusawa, J.L. Sørensen, S.L. Braunstein, C.A. Fuchs, H.J. Kimble, E.S. Polzik, Science **282**, 706 (1998)
15. J. Jing, J. Zhang, Y. Yan, F. Zhao, C. Xie, K. Peng, Phys. Rev. Lett. **90**, 167903 (2003)

16. T. Aoki, N. Takey, H. Yonezawa, K. Wakui, T. Hiraoka, A. Furusawa, P. van Loock, Phys. Rev. Lett. **91**, 080404 (2003)
17. M. Bondani, A. Allevi, E. Puddu, A. Andreoni, A. Ferraro, M.G.A. Paris, Opt. Lett. **29**, 180 (2004) and erratum **29**, 1417 (2004)
18. A.V. Rodionov, A.S. Chirkin, JETP Lett. **79**, 253 (2004)
19. A.S. Bradley, M.K. Olsen, O. Pfister, R.C. Pooser, Phys. Rev. A **72**, 053805 (2005)
20. M.K. Olsen, A.S. Bradley, J. Phys. B **39**, 127 (2006)
21. E.A. Mishkin, D.F. Walls, Phys. Rev. **185**, 1618 (1969); M.E. Smithers, E.Y.C. Lu, Phys. Rev. A **10**, 1874 (1974)
22. J. Guo, H. Zou, Z. Zhai, J. Zhang, J. Gao, Phys. Rev. A **71**, 034305 (2005)
23. N. Piovella, M. Cola, R. Bonifacio, Phys. Rev. A **67**, 013817 (2003)
24. S. Pirandola, S. Mancini, D. Vitali, P. Tombesi, Phys. Rev. A **68**, 062317 (2003)
25. G.X. Li, S.P. Wu, G.M. Huang, Phys. Rev. A **71**, 063817 (2005)
26. A. Allevi, M. Bondani, A. Ferraro, M.G.A. Paris, Laser Phys. **16**, 1451 (2006)
27. A. Agliati, M. Bondani, A. Andreoni, G. De Cillis, M.G.A. Paris, J. Opt. B: Quant. Semiclass. Opt. **7**, S652 (2005)
28. M. Bondani, A. Allevi, G. Zambra, M.G.A. Paris, A. Andreoni, Phys. Rev. A **76**, 013833 (2007)
29. D.T. Smithey, M. Beck, M.G. Raymer, A. Faridani, Phys. Rev. Lett. **70**, 1244 (1993)
30. A. Allevi, M. Bondani, M.G.A. Paris, A. Andreoni (in preparation)
31. M. Bondani, A. Allevi, E. Gevinti, A. Agliati, A. Andreoni, Opt. Express **14**, 9838 (2006)
32. F. Paleari, A. Andreoni, G. Zambra, M. Bondani, Opt. Express **12**, 2816 (2004)